ELSEVIER

Biochimica et Biophysica Acta 1283 (1996) 199–206

BBA Biochimica et Biophysica Acta

A calorimetric study of binary mixtures of saturated and monounsaturated mixed-chain phosphatidylethanolamines

Hai-nan Lin, Shusen Li, Guoquan Wang, Erich E. Brumbaugh, C. Huang *

Department of Biochemistry, Health Sciences Center, University of Virginia, Box 440, Charlottesville, VA 22908, USA

Received 29 January 1996; accepted 16 April 1996

Abstract

In this study, we have semisynthesized the following three molecular species of mixed-chain phosphatidylethanolamine: C(22):C(12)PE, C(16):C(18:1Δ^9)PE, and C(10):C(24:1Δ^{15})PE. These lipids share a common structural characteristic, that is, they all have the same total number of carbon atoms in their acyl chains. Aqueous dispersions prepared from three sets of binary lipid mixtures, C(16):C(18:1Δ^9)PE/C(22):C(12)PE, C(10):C(24:1Δ^{15})PE/C(22):C(12)PE, and C(16):C(18:1Δ^9)PE/C(10):C(24:1Δ^{15})PE, were studied by high-resolution differential scanning calorimetry, leading to the construction of three temperature-composition phase diagrams. A computer program developed on the basis of the thermodynamic equations for non-ideality of mixing (or Brigg-Williams approximation) was applied to fit the calorimetric data, yielding the non-ideality parameters of mixing in the gel and the liquid-crystalline bilayers (ρ^G and ρ^L). Based on the shapes of these phase diagrams and the values of ρ^G and ρ^L, it is concluded that any two of the three molecular species of phosphatidylethanolamines under study can mix nearly ideally in the bilayer plane of the liquid-crystalline bilayer. However, these binary lipid mixtures do exhibit the gel-gel phase immiscibility over an extensive compositional region in the gel-state bilayer. By comparison with experimental data obtained with binary mixtures of saturated identical-chain phospholipids, we can conclude that mixed-chain *cis*-monounsaturated lipid molecules and saturated lipid molecules are highly demixed in the same two-dimensional plane of the gel-state bilayer, although the bilayer thickness difference between the lipid bilayer composed of *cis*-monounsaturated lipids and that of saturated lipids may be only one or two C-C bond lengths at $T < T_m$.

Keywords: Binary lipid mixture; Differential scanning calorimetry; Mixed interdigitated bilayer; Phase diagram; Phase transition temperature

1. Introduction

Recently, we have applied the computer-based molecular mechanics (MM) computations and high-resolution differential scanning calorimetry (DSC) to study systematically the structures and melting properties of a large number of mixed-chain *cis*-monoenoic phospholipids in excess water [1–3]. More specifically, these are *sn*-1 saturated/*sn*-2 *cis*-monounsaturated phosphatidylcholines (PC) and phosphatidylethanolamines (PE) with chemical structures resembling those of naturally occurring membrane-phospholipids. Based on the computational and calorimetric data, some of the common structure/chain melting property relationships exhibited by most, if not all, mixed-chain *cis*-monoenoic phospholipids are delineated. For instance, the gel-to-liquid crystalline phase transition temperature, T_m, of the fully hydrated lipid bilayer prepared from single-component *cis*-monoenoic phospholipids is well known to be far below that for bilayers prepared from saturated counterparts. A good example is demonstrated by the bilayer composed of 1-stearoyl-2-oleoyl-phosphatidylcholines or C(18):C(18:1Δ^9)PC which, in excess water, exhibits calorimetrically a T_m value of 5.6°C [2]. In contrast, the T_m value of the fully hydrated bilayer composed of distearoyl phosphatidylcholines or C(18):C(18)PC is 55.3°C [4]. Despite the fact that the T_m-lowering effect of a single *cis* carbon-carbon double bond is well established, the fundamental mechanism underlying such a phenomenon remains to be elucidated. Our recent MM calculations indicate that in the gel-state bilayer, a single *cis*-double bond in the *sn*-2 acyl chain of a phosphatidylcholine molecule can cause the chain to kink in the shape of a crankshaft, resulting in two nearly parallel chain segments [5,6]. This structural information provides us a basis to formulate a model which can account for the T_m-lowering effect of a *cis*-double bond [3]. Our model can be briefly summarized as follows: the shorter segment of the kinked acyl chain is considered to

* Corresponding author. Fax: +1 (804) 9245069.

PII S0005-2736(96)00093-4

be partially disordered and, hence, it acts structurally as a perturbing element for the lateral lipid-lipid interactions. Moreover, since this shorter segment is already partially disordered at $T < T_m$, it does not contribute significantly to the conformational disordering process of *trans* → *gauche* isomerizations involved in the phase transition [3]. As a result, the total number of C-C *trans* bonds per lipid molecule undergoing the *trans* → *gauche* isomerization during the phase transition is decreased appreciably for the bilayer composed of *cis*-monoenoic phosphatidylcholines relative to that of the saturated counterparts, leading to a significantly lower T_m value.

After having studied extensively the phase transition behavior of single-component liposomes prepared from a large number of *cis*-monoenoic phospholipids, we now turn our attention to examine the thermal behavior of binary lipid mixtures containing *cis*-monoenoic phospholipids. Recently, some very interesting findings were reported from other laboratories concerning the mixing behavior of binary mixtures of saturated identical-chain phospholipids [7–9]. For instance, Snyder et al. [7] observed a small fraction of lipid demixing in the binary mixture of C(18):C(18)PC/C(20):C(20)PC at −19°C. However, the present knowledge about the mixing behavior of binary lipid mixtures containing *sn*-1 saturated/*sn*-2 *cis*-monounsatured phospholipids, particularly phosphatidylethanolamines, is still scanty. Hence, in this study three molecular species of mixed-chain phosphatidylethanolamine including one saturated mixed-chain phosphatidylethanolamine and two *sn*-1 saturated/*sn*-2 *cis*-monounsaturated phosphatidylethanolamines were first semisynthesized. These three lipids have the same total number of carbon atoms in their acyl chains. Subsequently, the thermal behavior of binary mixtures of these semisynthesized lipids was studied calorimetrically. Based on the calorimetric data, three temperature-composition phase diagrams were constructed using Brumbaugh's simulation program [10]. Analyses of these phase diagrams showed that *cis*-monoenoic phospholipids in the gel-state bilayer are significantly demixed from the saturated phospholipids. Earlier, we have proposed that the short chain segment of the kinked *sn*-2 acyl chain in the *sn*-1 saturated/*sn*-2 *cis*-monounsaturated phospholipid molecule acts as a perturbing element in the gel-state bilayer which can account for the T_m-lowering effect of a *cis*-double bond [3]. Now, we suggest that this perturbing element is also responsible for the demixing behavior exhibited by *cis*-monoenoic phospholipids in the gel-state bilayer.

2. Materials and methods

2.1. Materials and semisynthesis of phosphatidylethanolamines

Various saturated and monounsaturated fatty acids were purchased from Sigma (St. Louis, MO). Lysophosphatidylcholines were provided by Avanti Polar Lipids (Alabaster, AL). These fatty acids and lysolipids were used as the starting materials to semisynthesis mixed-chain phosphatidylcholines, at room temperature, using the modified procedure of Mena and Djerassi [11] as described previously [12]. Each of the synthesized mixed-chain phosphatidylcholines was subsequently converted enzymatically to the corresponding mixed-chain phosphatidylethanolamine by the transphosphatidylation with phospholipase D in the presence of excess amount of ethanolamine hydrochloride, at pH 5.6, as described in detail elsewhere [13]. In this study, three molecular species of mixed-chain phosphatidylethanolamine were semisynthesized; they were 1-palmitoyl-2-oleoyl-phosphatidylethanolamine (C(16):C(18:1Δ^9)PE), 1-capryl-2-nervonoyl-phosphatidylethanolamine (C(10):C(24:1Δ^{15})PE), and 1-behenoyl-2-lauroyl-phosphatidylethanolamine (C(22):C(12)PE). After semisynthesis, various mixed-chain phospholipids were purified by repeated column chromatography on Silica gel 60 (Mesh numbers:230-400), eluting with chloroform/methanol mixtures as reported earlier [12]. The purified phospholipids were analyzed by TLC with $CHCl_3/CH_3OH/NH_4OH$ (65:30:5); only a single spot was observed for each molecular species of phosphatidylethanolamine at a loading of about 1 μmol per sample. In addition, the high purity of the semisynthesized phosphatidylethanolamine was established further by the single, sharp endothermic peak observed in the differential scanning calorimetric scan.

2.2. DSC measurements

Prior to high-resolution differential scanning calorimetry (DSC) experiments, binary lipid mixtures of C(16):C(18:1Δ^9)PE/C(22):C(12)PE, C(10):C(24:1Δ^{15})PE/C(22):C(12)PE, and C(16):C(18:1Δ^9)PE/C(10):C(24:1Δ^{15})PE with various concentration ratios were prepared in 50 mM NaCl solution containing 5 mM phosphate buffer, 1 mM EDTA and 0.02 mg/ml NaN_3 (pH 7.4), according to the method of Lin and Huang [14]. These lipid samples were preincubated at 4°C under N_2 atmospheres for a minimum of 24 h prior to DSC scans.

DSC experiments were performed using a high-resolution Microcal microcalorimeter (Model MC-2) equipped with DA-2 digital interface and data acquisition utility for automatic data collection (Microcal, Northampton, MA). In all DSC experiments, a constant heating/cooling scan rate of 15°C/h was used. The construction of the phase diagram was based on the DSC heating curves for a given binary mixture at various relative compositions, following the procedure described earlier [14]. Briefly, the onset and completion temperatures for each transition peak, after proper correction for the finite widths of the transition peaks of the pure components [15], were plotted as a

function of the mole fraction of the higher melting component lipid. These corrected onset and completion temperature points form the bases for defining the solidus and liquidus, respectively, of the temperature-composition phase diagram.

2.3. Simulations of the phase diagrams

The basic thermodynamic equations, derived from the regular solution theory (or Brigg-Williams approximation), describing phenomenologically the phase diagram of non-ideal binary mixtures of phospholipid components A and B in the two-dimensional plane of the bilayer are given below [16]:

$$\ln\left(X_B^G/X_B^L\right) = \Delta H_B/R(1/T - 1/T_B) + 1/RT\left[\rho^L\left(1-X_B^L\right)^2 - \rho^G\left(1-X_B^G\right)^2\right] \quad (1)$$

$$\ln\left[\left(1-X_B^G\right)/\left(1-X_B^L\right)\right] = \Delta H_A/R(1/T - 1/T_A) + 1/RT\left[\rho^L\left(X_B^L\right)^2 - \rho^G\left(X_B^G\right)^2\right] \quad (2)$$

where X_B^G and X_B^L, the composition variables, are the mole fraction of the high melting component B in the gel and liquid-crystalline phases, respectively, ΔH_A and ΔH_B are the transition enthalpies (kcal/mol) of pure components A and B, respectively, T_A and T_B are the phase transition temperatures (Kelvin) of the bilayers composed of the pure components A and B, respectively, and ρ^G and ρ^L are two parameters having units of energy (kcal/mol) which describe the nonideality of mixing between components A and B in the gel and liquid-crystalline phases of the bilayer, respectively. The nonideality parameter, ρ, is related to the pair-interaction energy between mixed pairs and between like pairs in the two dimensional plane of the bilayer as follows: $\rho = Z[E_{AB} - 1/2\,(E_{AA} + E_{BB})]$, where Z is the number of nearest neighbors in the plane of the bilayer, and E_{AB}, E_{AA}, and E_{BB} are the molar interaction energies of A-B, A-A, B-B pairs of nearest neighbor pairs, respectively [16,17]. If the value of ρ is positive, then there is a tendency for like-lipid species to cluster together leading to lateral phase separation; $\rho < 0$ reflects the tendency of compound formation; $\rho = 0$ corresponds to ideal lateral mixing between components A and B in the bilayer.

Eq. (1) and Eq. (2) allow the shape of the phase diagram for a given binary lipid mixture to be determined, provided that the values of ρ^L and ρ^G and other experimental values (T_m and ΔH) are known. On the other hand, if the shape of the phase diagram has already been determined experimentally, Eq. (1) and Eq. (2) can be used to estimate the ρ^L and ρ^G values by matching the experimental and the simulated phase diagrams [18,19]. A computer simulation program utilizing the statistical method of nonlinear least-squares was developed in this laboratory by Brumbaugh to determine the ρ^L and ρ^G values based on the experimental data and Eq. (1) and Eq. (2) [10]. The ρ^L and ρ^G values reported in this communication were obtained using Brumbaugh's program. Briefly, two rounds of simulations were generally carried out. In the first round, all experimental values (T_m and ΔH) were fixed, and the phase diagram was simulated by adjusting simultaneously the ρ^L and ρ^G values in such a way that the shape of the simulated phase diagram can match reasonably well with the experimentally determined solidus and liquidus. In the second round, all or selected T_m and ΔH values and the ρ values from round one were allowed to float during the matching process, leading to a refined phase diagram with a reduction in variance.

3. Results

3.1. The phase diagram for C(16):C(18:1Δ⁹)PE / C(22):C(12)PE mixtures

The thermal behavior of a series of aqueous dispersions prepared individually from C(16):C(18:1Δ⁹)PE/

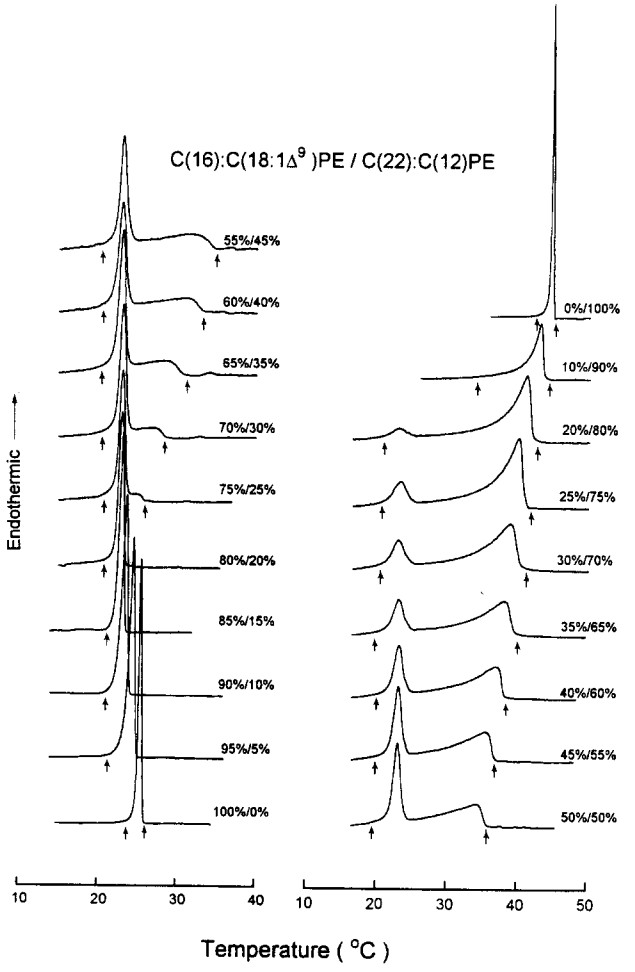

Fig. 1. The second DSC heating thermograms for samples of C(16):C(18:1Δ⁹)PE/C(22):C(12)PE mixtures containing various mole fractions as indicated. The onset and completion temperatures for each phase transition curve are indicated by arrows.

C(22):C(12)PE mixtures with different concentration ratios was studied calorimetrically as a function of temperature. The observed DSC heating curves for the binary mixtures with increasing C(22):C(12)PE content are summarized in Fig. 1, in which the onset and completion temperatures of the endothermic transition are indicated by arrows. The aqueous dispersion of the pure C(16):C(18:1Δ^9)PE exhibits a single, sharp, reasonably symmetrical transition peaked at 26.1°C (T_m) with a transition enthalpy (ΔH) of 5.4 kcal/mol and a peak-width at half maximal height ($\Delta T_{1/2}$) of 0.5°C. Interestingly, the values of T_m and ΔH obtained from the first DSC heating scan of the pure C(16):C(18:1Δ^9)PE sample, which has been preincubated at 4°C for 24 h, are reproducible upon immediately repeated reheatings, indicating that the chain melting characteristics of the bilayer are independent of the thermal history.

As the relative content of C(22):C(12)PE in the binary mixture of C(16):C(18:1Δ^9)PE/C(22):C(12)PE increases from 0 to 20 mol%, the transition curves for the binary mixtures are characterized by single endothermic peaks; however, the transition curves are slightly broadened and the T_m values are gradually down-shifted (Fig. 1). At 25 mol% of C(22):C(12)PE, the binary mixture exhibits a main endothermic transition with a high-temperature shoulder. As the relative content of C(22):C(12)PE continues to increase progressively up to 80 mol%, the magnitude of the transition peak originated from the pure C(16):C(18:1Δ^9)PE decreases successively. On the other hand, the shoulder appeared in the transition peak for the binary mixture containing 25 mol% C(22):C(12)PE grows and shifts gradually to higher temperatures. Above 80 mol% of C(22):C(12)PE, the DSC curves are again characterized by single endothermic peaks with nearly symmetric shapes. For 100% C(22):C(12)PE, the single, narrow, nearly symmetric peak has a T_m of 44.7°C with a $\Delta T_{1/2}$ of 0.4°C and a ΔH of 12.4 kcal/mol. Most interestingly, this T_m value is only 1.6°C higher than that of the C(22):C(12)PC bilayer [20]. This small difference in T_m between the C(22):C(12)PE bilayer and the C(22):C(12)PC bilayer can be taken as evidence indicating that C(22):C(12)PEs are self-assembled, in excess water and at $T < T_m$, into the gel-state bilayer with a mixed interdigitated packing motif [21]. Such a structural motif has been detected experimentally for the fully hydrated C(22):C(12)PC bilayer, at $T < T_m$, by Zhu and Caffrey [22].

In Fig. 2, the corrected onset and completion temperatures for each transition curve shown in Fig. 1 are plotted as a function of C(22):C(12)PE content. The lines connecting the corrected onset and completion temperatures are the solidus and liquidus, respectively, of the simulated phase diagram for C(16):C(18:1Δ^9)PE/C(22):C(12)PE mixtures. The simulation uses Brumbaugh's program with $\rho^G = 1.30$ and $\rho^L = 0.00$ kcal/mol. It is evident from Fig. 2 that the simulated phase diagram fits the experimental data very well; moreover, the phase diagram has the shape of a eutectic system. This eutectic phase diagram is characterized by the eutectic point at 16.5 mol% of C(22):C(12)PE and 22.0°C. Another key feature of the eutectic phase

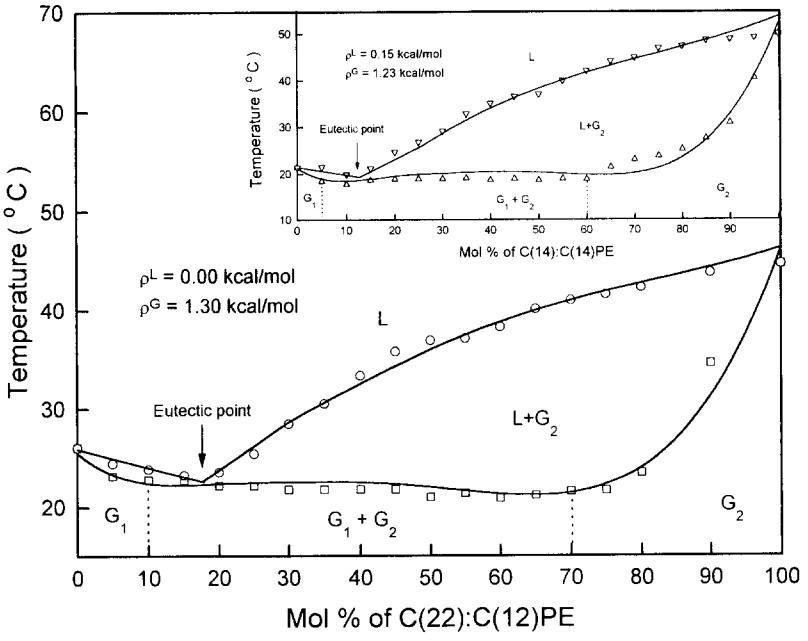

Fig. 2. The temperature-composition phase diagram for C(16):C(18:1Δ^9)PE/C(22):C(12)PE mixtures. The experimental data points are the corrected onset and completion temperatures of the various transition peaks shown in Fig. 1. The solidus and liquidus of the phase diagram are obtained from the computer-simulation program of Brumbaugh [10]; however, the temperatures are expressed in °C. G_1, the C(16):C(18:1Δ^9)PE enriched phase; G_2, the C(22):C(12)PE enriched gel phase; L, the liquid-crystalline phase. The inset shows the phase diagram for C(18):C(10)PE/C(14):C(14)PE mixtures [22]. The dotted lines are estimated solvus lines.

diagram shown in Fig. 2 is the long eutectic horizontal which spans the composition range from 10 to 70 mol% C(22):C(12)PE and occurs at 21.5 ± 0.5°C. Below the eutectic horizontal is a two-phase immiscible region in which the C(16):C(18:1Δ^9)PE enriched domain and the C(22):C(12)PE enriched domain co-exist in equilibrium. The small amount of C(22):C(12)PE present in the C(16):C(18:Δ^9)PE enriched domain can be considered as a minor component of impurity, and vice versa for the C(22):C(12)PE enriched domain. Above the liquidus, binary mixtures of C(16):C(18:1Δ^9)PE/C(22):C(12)PE are mixed ideally and homogeneously in all proportions to form a single liquid-crystalline phase (L), as indicated by the ρ^L value of zero. It is worth pointing out that the overall shape of the phase diagram for C(16):C(18:1Δ^9)PE/C(22):C(12)PE mixtures is remarkably similar to that exhibited by C(18):C(10)PE/C(14):C(14)PE mixtures [21]. As a reference, the phase diagram for C(18):C(10)PE/C(14):C(14)PE mixtures is shown in the inset in Fig. 2. In this case, the ρ^L and ρ^G are determined to be 0.15 and 1.23 kcal/mol, respectively. The ρ^L value of 0.15 kcal/mol is, in fact, smaller than the average kinetic energy of the thermal environment at room temperature (0.58 kcal/mol); hence, the two lipid components, C(18):C(10)PE and C(14):C(14)PE, are mixed nearly ideally in the liquid-crystalline state at room temperature.

3.2. The phase diagram for C(10):C(24:1Δ^{15})PE / C(22):C(12)PE mixture

After examining the eutectic phase diagram for C(16):C(18:1Δ^9)PE/C(22):C(12)PE mixtures, we studied the thermal behavior of C(10):C(24:1Δ^{15})PE/C(22):C(12)PE mixtures. This *cis*-monoenoic phospholipid, C(10):C(24:1Δ^{15})PE, is highly asymmetrical with a ΔC/CL value of 0.56. Similarly, the C(22):C(12)PE molecule has a ΔC/CL value of 0.55. The ratio ΔC/CL is a structural parameter describing the asymmetry of lipid acyl chains in the gel state bilayer [3,23]; the larger the ratio, the more asymmetrical the lipid molecule. When the value of ΔC/CL is determined for a lipid molecule to be 0.56, it means that the longer acyl chain of the phospholipid molecule is about twice as long as the shorter acyl chain of the same lipid molecule. The DSC curve for the aqueous dispersion of pure C(10):C(24:1Δ^{15})PE is shown in Fig. 3A as the bottom-most trace. The phase transition exhibited by the C(10):C(24:1Δ^{15})PE bilayer is characterized by a highly cooperative endotherm peaked at 27.3°C (T_m) with a $\Delta T_{1/2}$ value of 0.4°C and a ΔH value of 5.8 kcal/mol. Moreover, the transition behavior is independent of the thermal history of the sample.

Traces of DSC curves for C(10):C(24:1Δ^{15})PE/C(22):C(12)PE mixtures at 11 different concentration ratios are presented in Fig. 3A. The simulated phase diagram obtained from Brumbaugh's program based on the corrected onset and completion temperatures for each of the transitions shown in Fig. 3A is summarized in Fig. 3B. This simulation yields $\rho^G = 1.08$ and $\rho^L = 0.28$ kcal/mol.

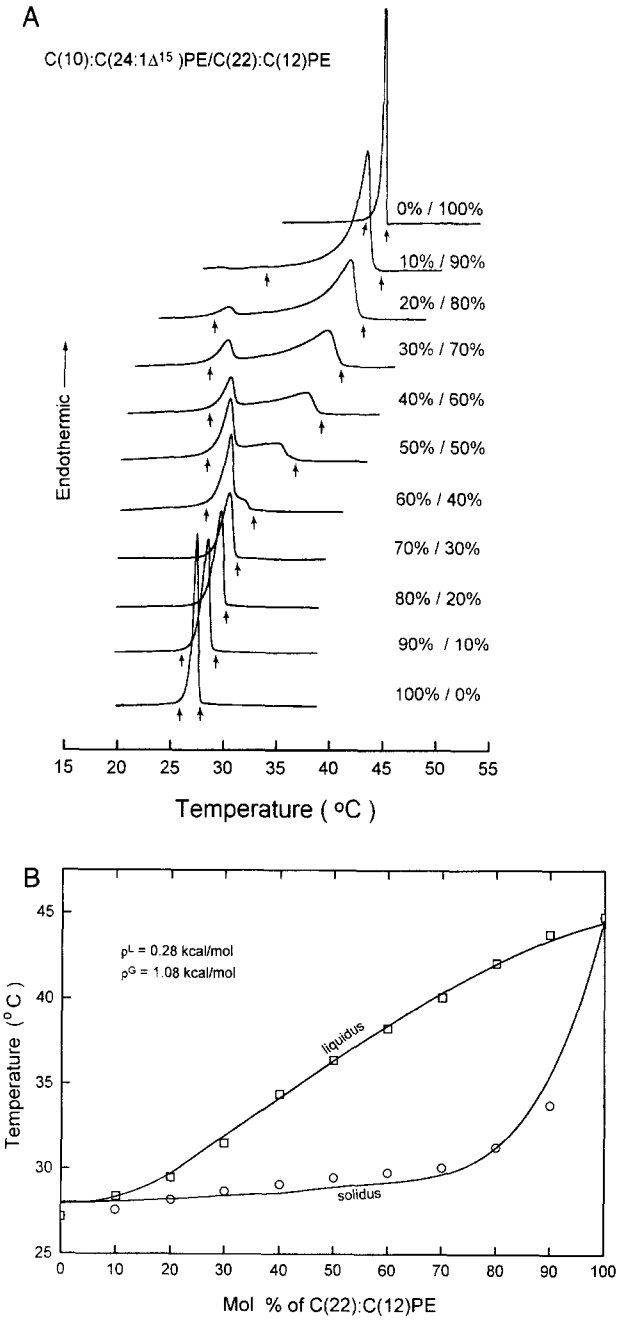

Fig. 3. The phase transition behavior exhibited by binary mixtures of C(10):C(24:1Δ^{15})PE/C(22):C(12)PE. (A) The second DSC heating curves of the binary mixture recorded at different molar ratios of the component lipids as indicated. (B) The phase diagram obtained with the computer-simulation program of Brumbaugh [10].

3.3. The phase diagram for C(16):C(18:1Δ^9)PE / C(10):C(22:1Δ^{15})PE mixtures

After constructing the two phase diagrams for C(16):C(18:1Δ^9)PE/C(22):C(12)PE and

C(10):C(24:1Δ^{15})PE/C(22):C(12)PE mixtures, we studied the final set of binary mixtures composed of C(16):C(18:1Δ^{9})PE and C(10):C(24:1Δ^{15})PE. These two *cis*-monoenoic lipid species, C(16):C(18:1Δ^{9})PE and C(10):C(24:1Δ^{15})PE, have the same MW. However, the $\Delta C/CL$ values for the two *cis*-monoenoic lipid molecules are 0.02 and 0.56, respectively. Fig. 4 shows twenty DSC heating curves for aqueous dispersions of C(16):C(18:1Δ^{9})PE/C(10):C(24:1Δ^{15})PE mixtures containing different contents. As the mol% of C(10):C(24:1Δ^{15})PE incorporated into C(16):C(18:1Δ^{9})PE bilayers increases from 0 to 35, the T_m of the phase transition in the DSC heating curve is observed in Fig. 4 to decrease progressively; however, the transition peak-width broadens initially up to 12.5 mol% of C(10):C(24:1Δ^{15})PE and thereafter it narrows successively. As the mol% of C(10):C(22:1Δ^{15})PE increases continuously from 40 to 100, a reverse trend in T_m is observed, that is, the T_m increases with increasing content of C(10):C(22:1Δ^{15})PE. Moreover, the width of the transition peak broadens progressively up to 80 mol% and then narrows steadily as the content reaches 100 mol% C(10):C(24:1Δ^{15})PE.

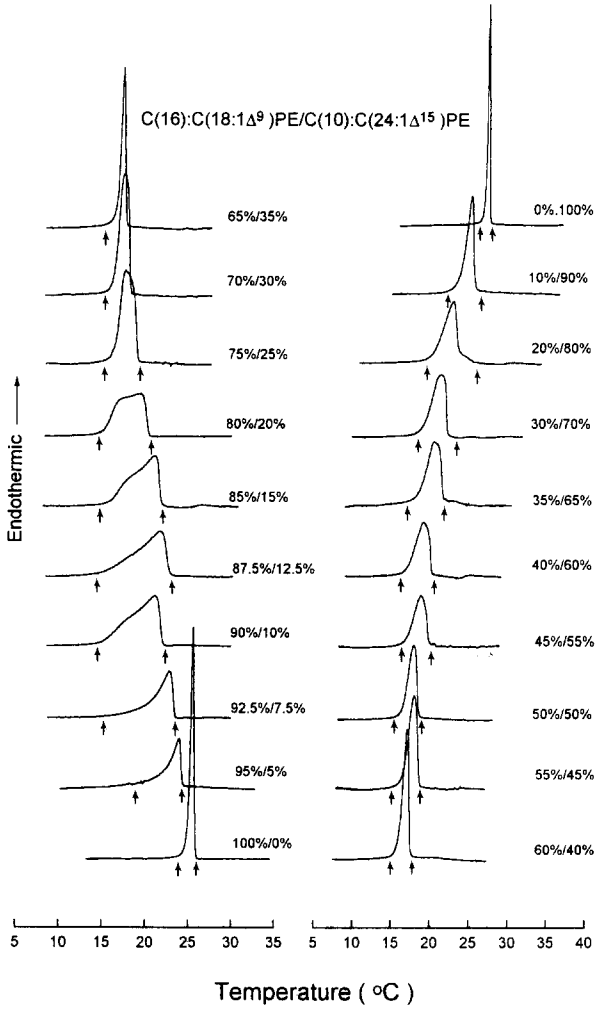

Fig. 4. The second DSC heating curves for samples of C(16):C(18:1Δ^{9})PE/C(10):C(24:1Δ^{15})PE mixtures containing various molar ratios of the component lipids as indicated.

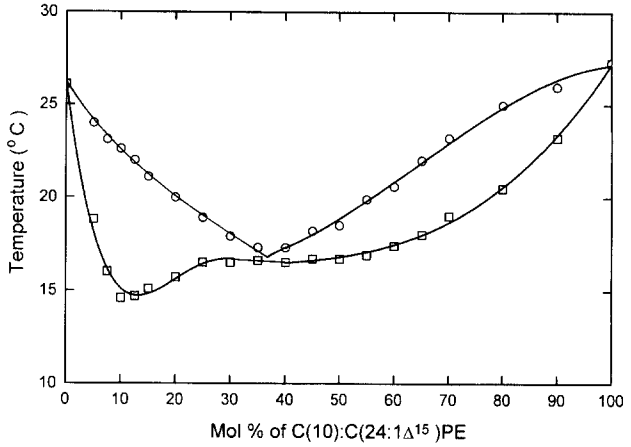

Fig. 5. The hand-drawn phase diagram for C(16):C(18:1Δ^{9})PE/C(10):C(24:1Δ^{15})PE mixtures. The experimental data points are the corrected onset and completion temperatures of the phase transition curves shown in Fig. 4.

The phase diagram for C(16):C(18:1Δ^{9})PE/C(10):C(24:1Δ^{15})PE mixtures are presented in Fig. 5. The lines connecting the corrected onset and completion temperatures are hand-drawn, since the shape of the phase diagram cannot be simulated satisfactorily by Brumbaugh's simulation program with any pair of ρ^G and ρ^L values. The difficulty lies in the solidus. Specifically, the simulated line attempted to match the corrected onset temperatures cannot fit the experimental data points lying in between 10 and 25 mol% of C(10):C(24:1Δ^{15})PE. Despite the lack of simulated ρ values, the shape of the hand-drawn phase diagram resembles that of a eutectic phase diagram.

4. Discussion

The miscibility/immiscibility of two phospholipid species A and B in the bilayer as revealed by the phase diagram depends on the relative strength of the lateral lipid-lipid interactions (A-B, A-A, and B-B pairs) in the two-dimensional plane of the bilayer which, in turn, can be expected to depend on the structural characteristics of the molecular species A and B. It is thus important to consider the structural characteristics of the component phospholipid species prior to the analysis of the phase diagram.

The two acyl chains of C(16):C(18:1Δ^{9})PE are nearly identical in length; hence, this *cis*-monoenoic lipid species is characterized by a rather small $\Delta C/CL$ value of 0.03. Symmetric and moderately asymmetric phospholipids with $\Delta C/CL$ values less than 0.4 are usually assembled, at $T < T_m$, into the normal gel-state bilayer with a partially interdigitated packing motif [24]. For the C(16):C(18:1Δ^{9})PE gel-state bilayer, the thickness of the hydrocarbon core (N), which is the distance separating the

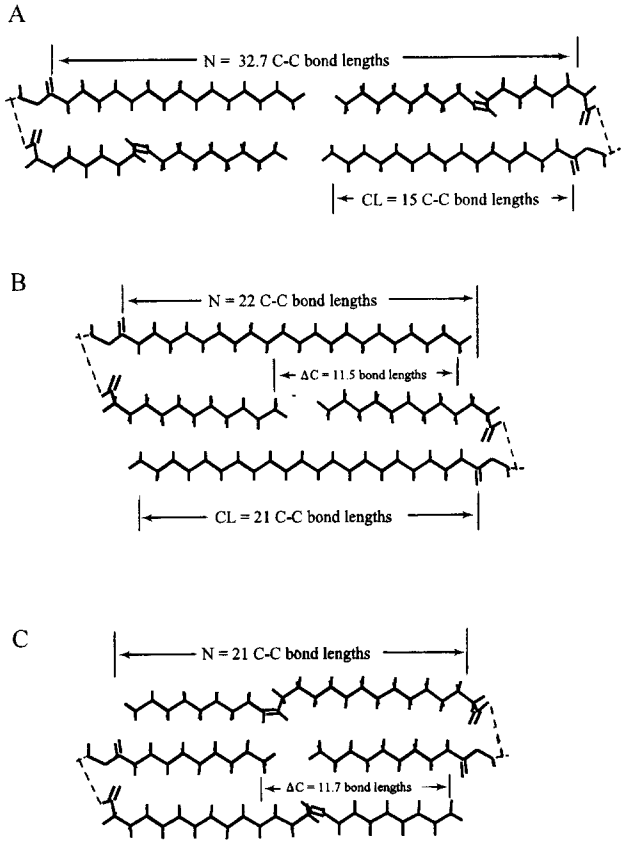

Fig. 6. Schematic diagrams showing the packing motif, at $T < T_m$, of a trans-bilayer dimer for (A) C(16):C(18:1Δ^9)PE, (B) C(22):C(12)PE, and (C) C(10):C(24:1Δ^{15})PE. N, the thickness of the hydrocarbon core; ΔC, the effective acyl chain length difference between the *sn*-1 and *sn*-2 acyl chains; CL, the effective chain length of the longer acyl chain. In these figures, only the diglyceride moiety of the PE molecule is illustrated diagrammatically.

two carbonyl oxygens of the two opposing *sn*-1 acyl chains in the trans-bilayer dimer (Fig. 6A), can be estimated to be about 32.7 C-C bond lengths, when the monoenoic *sn*-2 acyl chain is assumed to adopt a crankshaft-like kink conformation in the normal gel-state bilayer [3]. In contrast, highly asymmetric C(22):C(12)PE and C(10):C(24:1Δ^{15})PE with a nearly identical $\Delta C/CL$ value of 0.55–0.56 can be reasonably assumed to self-assemble, in excess water, into the mixed interdigitated bilayer at $T < T_m$ (Fig. 6B,C). The thickness of the hydrocarbon core (N) for the mixed interdigitated gel-state bilayers are 22 and 21 C-C bond lengths for C(22):C(12)PE and C(10):C(24:1Δ^{15})PE, respectively [21].

The large difference in the N-value between the C(16):C(18:1Δ^9)PE bilayer and the C(22):C(12)PE or C(10):C(24:1Δ^{15})PE bilayer, at $T < T_m$, can be taken as a major reason for the eutectic phase diagrams observed in Figs. 2 and 5. For instance, the Van der Waals' contact surface between the two neighboring trans-bilayer dimers of C(16):C(18:1Δ^9)PE in the two dimensional plane of the gel-state bilayer is significantly larger than that between the two neighboring trans-bilayer dimers of C(22):C(12)PE due to the larger N-value for the C(16):C(18:1Δ^9)PE bilayer. Consequently, a stronger lateral lipid-lipid interaction is expected between the two trans-bilayer dimers of C(16):C(18:1Δ^9)PE in the gel-state bilayer. This stronger lateral lipid-lipid interaction will promote the aggregation of C(16):C(18:1Δ^9)PEs, leading to the domain formation of separated gel phases. The separation of the gel-state C(16):C(18:1Δ^9)PE enriched domain from the C(22):C(12)PE enriched gel-domain as seen in the phase diagram (Fig. 2) under the eutectic horizontal can thus be rationalized. Similarly, the disparity in the bilayer thickness between the C(10):C(24:1Δ^{15})PE and the C(16):C(18:1Δ^9)PE bilayers at $T < T_m$ can explain, in part, the eutectic phase diagram shown in Fig. 5 for C(10):C(24:1Δ^{15})PE/C(16):C(18:1Δ^9)PE mixtures.

In the liquid-crystalline state, highly asymmetric phospholipid molecules can undergo rapid dynamic motions in each of the two monolayers within the bilayer. For instance, highly asymmetric C(18):C(10)PCs ($\Delta C/CL = 0.56$) at $T < T_m$ adopt the mixed interdigitated packing motif in the gel-state bilayer; interestingly, at $T > T_m$ these highly asymmetric lipid molecules undergo rapid lateral diffusions in the plane of the liquid-crystalline bilayer. In fact, the averaged rate of lateral diffusion observed for C(18):C(10)PC molecules in the liquid-crystalline bilayer is identical to that observed for identical-chain C(14):C(14)PC molecules in the liquid-crystalline bilayer [25]. It should be pointed out that C(18):C(10)PC and C(14):C(14)PC have the same total number of carbon atoms in their two acyl chains, and they form liquid-crystalline bilayers with the same thickness [24]. Similarly, C(16):C(18:1Δ^9)PE, C(22):C(12)PE, and C(10):C(24:1Δ^{15})PE share a common total number of carbon atoms in their acyl chains. Based on what we know about C(18):C(10)PC and C(14):C(14)PC [24,25], it can be reasonably inferred that the three molecular species of phosphatidylethanolamines under study probably can also undergo rapid lateral diffusions with a nearly common diffusion rate in the bilayer plane at $T > T_m$. As a consequence, a nearly ideal mixing between any pair of the three lipid species can be expected to occur in the liquid-crystalline bilayer. This expectation is indeed borne out by the simulated ρ^L values for the phase diagrams shown in Figs. 2 and 3B. The eutectic phase diagram shown in Fig. 5 also indicates a nearly ideal mixing between the two component lipids in the liquid-crystalline bilayer.

Recently, experimental results obtained with binary mixtures of C(18):C(18)PC/C(20):C(20)PC by infrared studies indicated that only 4 mol% of C(20):C(20)PC aggregated into gel domains at −19°C [7,8]. The difference in the bilayer thickness between the gel-state C(18):C(18)PC and C(20):C(20)PC bilayers is 4 C-C bond lengths. In a separate DSC study of fully hydrated C(16):C(16)PE/C(18):C(18)PE mixtures, a lens-shaped phase diagram with a ρ^G value of 0.54 kcal/mol was observed [9], indicating nearly ideal mixing of the two

component lipids in the gel-state bilayer. The difference in the bilayer thickness between the gel-state C(16):C(16)PE and C(18):C(18)PE bilayers is also 4 C-C bond lengths. In view of these recent observations, the extensive gel-gel phase immiscibility and the ρ^G value of 1.08 kcal/mol for C(10):C(24:1Δ^{15})PE/C(22):C(12)PE mixtures shown in Fig. 3B appear to be unusual, since the C(10):C(24:1Δ^{15})PE and C(22):C(12)PE bilayers, at $T < T_m$, share a common packing motif of mixed interdigitation and the difference in the effective bilayer thickness between them is only one C-C bond length (Fig. 6). However, it must be emphasized that C(10):C(24:1Δ^{15})PE is a *cis*-monoenoic phosphatidylethanolamine molecule in which a *cis*-double bond is present in the *sn*-2 acyl chain, whereas the various lipids employed in the recent infrared and DSC studies cited above are all saturated identical-chain phospholipids. For *cis*-monoenoic phospholipids packed in the gel-state bilayer, the single *cis* double bond in the *sn*-2 acyl chain can kink the *sn*-2 acyl chain of the lipid molecule into two linear segments [5,6]. Moreover, the shorter segment in the kinked chain is considered to be disordered at temperatures below the T_m; hence, it acts structurally at $T < T_m$ as a perturbing element in the lateral lipid-lipid interactions [3]. The disordered segments of the *sn*-2 acyl chains in C(10):C(24:1Δ^{15})PEs can, therefore, hinder the close encounters of C(22):C(12)PEs in the gel-state bilayer, thus promoting the domain formation of C(22):C(12)PE molecules and the gel-gel phase separation. Consequently, the gel-gel phase immiscibility shown in Fig. 3B can be attributed to the disordering effect of the shorter segment of the *sn*-2 acyl chain in C(10):C(24:1Δ^{15})PE. It should be mentioned at this point that the phase diagram for C(16):C(18:1Δ^9)PC/C(16):C(16)PC mixtures has been determined calorimetrically [26]. Although the difference in the bilayer thickness between the gel-state C(16):C(18:1Δ^9)PC and C(16):C(16)PC bilayers is about 2 C-C bond lengths, the shape of this phase diagram is that of a peritectic system, indicating an extensive region of immiscibility between the two lipids components in the gel-state bilayer. This gel-gel phase immiscibility can be explained similarly by the presence of the perturbing element in the kinked *sn*-2 acyl chain of C(16):C(18:1Δ^9)PC in the gel-state bilayer. Finally, based on the shapes of the phase diagrams of C(10):C(24:1Δ^{15})PE/C(22):C(12)PE and C(16):C(18:1Δ^9)PC/C(16):C(16)PC mixtures, we can conclude that in the two-dimensional plane of the gel-state bilayer, *cis*-monounsaturated and saturated phospholipid molecules are demixed significantly.

Acknowledgements

This research was supported, in part, by U.S. Public Health Service Grant GM-17452 from NIH. We are grateful to Mrs. Debbie Londeree Proffitt for typing this manuscript during the difficult times while the effect of the blizzard of '96 was lingering on.

References

[1] Wang, Z-q., Lin, H-n., Li, S. and Huang, C. (1994) J. Biol. Chem. 269, 23491–23499.
[2] Wang, Z-q., Lin, H-n., Li, S. and Huang, C. (1995) J. Biol. Chem. 270, 2014–2023.
[3] Wang, G., Lin, H-n., Li, S. and Huang, C. (1995) J. Biol. Chem. 270, 22738–22746.
[4] Huang, C., Wang, Z-q., Lin, H-n., Brumbaugh, E.E. and Li, S. (1994) Biochim. Biophys. Acta 1189, 7–12.
[5] Li, S., Lin, H-n., Wang, Z-q. and Huang, C. (1994) Biophy. J. 66, 2005–2018.
[6] Huang, C. and Li, S. (1996) in Handbook of Nonmedical Applications of Liposomes, Vol. 1 (Lasic, D.D. and Barenholz, Y., eds), pp. 173–194, CRC Press, Boca Raton, FL.
[7] Snyder, R.G., Strauss, H.L. and Cates, D.A. (1995) J. Phys. Chem. 99, 8432–8439.
[8] Mendelsohn, R., Liang, G.L., Strauss, H.L. and Snyder, R. G. (1995) Biophys. J. 69, 1987–1998.
[9] Nibu, Y. and Inoue, T. (1995) Chem. Phys. Lipids 76, 159–169.
[10] Brumbaugh, E.E. and Huang, C. (1992) Meth. Enzymol. 210, 531–539.
[11] Mena, P.L. and Djerassi, C. (1985) Chem. Phys. Lipids 37, 257–270.
[12] Lin, H-n., Wang, Z-q. and Huang, C. (1990) Biochemistry 29, 7063–7072.
[13] Xu, H., Stephenson, F.A., Lin, H-n. and Huang, C. (1988) Biochim. Biophys. Acta 943, 63–75.
[14] Lin, H-n. and Huang, C. (1988) Biochim. Biophys. Acta 946, 178–184.
[15] Mabrey, S. and Sturtevant, J.M. (1976) Proc. Natl. Acad. Sci. USA 73, 3862–3866.
[16] Lee, A.G. (1977) Biochim. Biophys. Acta 472, 285–344.
[17] Tenchov, B.G. (1985) Prog. Surf. Sci. 20, 273–340.
[18] Davis, P.J. and Keough, K.M.W. (1984) Chem. Phys. Lipids 25, 299–308.
[19] Brumbaugh, E.E., Johnson, M.L. and Huang C. (1990) Chem. Phys. Lipids 52, 69–78.
[20] Li, S., Wang, Z-q., Lin, H-n. and Huang, C. (1994) Biochim. Biophys. Acta 1194, 271–280.
[21] Lin, H-n., Li, S., Brumbaugh, E.E. and Huang, C. (1995) Arch. Biochem. Biophys. 319, 408–412.
[22] Zhu, T. and Caffrey, M. (1993) Biophys. J. 65, 939–954.
[23] Mason, J.T., Huang, C. and Biltonen, R.L. (1981) Biochemistry 20, 6086–6092.
[24] Huang, C. (1990) Klin Wochenschrift 68, 149–165.
[25] Schram, V. and Thompson, T.E. (1995) Biophys. J. 69, 2517–2520.
[26] Curatolo, W., Sears, B., Neuringer, L.J. (1985) Biochim. Biophys. Acta 817, 261–270.